Original Article

Comparison of the diagnostic accuracy between ^{18}F-FAPI-04 PET/CT and ^{18}F-FDG PET/CT in the clinical stage IA of lung adenocarcinoma

Han-Xiang Liang[1,2#], Qi-Wen Huang[3#], Yue-Mei He[4#], Yuan-Qi Mai[5], Zhe-Lin Chen[6], Bao-Ping Wang[7], Ning Fang[8], Jian-Feng Hu[9], Xie Li[2], Ning Zhang[2], En-Tao Liu[10], Xin-Chun Li[1,9]

[1]The First Affiliated Hospital of Jinan University, Guangzhou, China; [2]Department of Nuclear Medicine, Maoming People's Hospital, Maoming, China; [3]Department of Pathology, Maoming People's Hospital, Maoming, China; [4]Center of Scientific Research, Maoming People's Hospital, Maoming, China; [5]Department of Radiology, Maoming People's Hospital, Maoming, China; [6]Department of Cardiology, Maoming People's Hospital, Maoming, China; [7]Department of Neurology, The Air Force Hospital of Southern Theater Command, Guangzhou, China; [8]Department of Thoracic Surgery, Maoming People's Hospital, Maoming, China; [9]Department of Radiology, The First Affiliated Hospital of Guangzhou Medical University, Guangzhou, China; [10]PET Center, Department of Nuclear Medicine, Guangdong Provincial People's Hospital (Guangdong Academy of Medical Sciences), Southern Medical University, Guangzhou, China

Contributions: (I) Conception and design: HX Liang, YM He, YQ Mai, ET Liu, XC Li; (II) Administrative support: ET Liu, XC Li; (III) Provision of study materials or patients: QW Huang, N Fang, JF Hu, ZL Chen, BP Wang; (IV) Collection and assembly of data: QW Huang, HX Liang, JF Hu, N Fang, X Li, ZL Chen, BP Wang; (V) Data analysis and interpretation: YM He, HX Liang; (VI) Manuscript writing: All authors; (VII) Final approval of manuscript: All authors.

[#]These authors contributed equally to this work.

Correspondence to: En-Tao Liu, MD. PET Center, Department of Nuclear Medicine, Guangdong Provincial People's Hospital (Guangdong Academy of Medical Sciences), Southern Medical University, 106 Zhongshan Er Road, Yuexiu District, Guangzhou 510080, China. Email: liuentao@gdph.org.cn; Xin-Chun Li, MD. The First Affiliated Hospital of Jinan University, Guangzhou, China; Department of Radiology, The First Affiliated Hospital of Guangzhou Medical University, No. 151 Yan-Jiang West Road, Yuexiu District, Guangzhou 510120, China. Email: xinchunli@163.com.

Background: Fluorine 18-labeled fibroblast activation protein inhibitor (^{18}F-FAPI-04) positron emission tomography/computed tomography (PET/CT) has shown promise for the visualization of advanced stage lung cancer. The accuracy of ^{18}F-FAPI-04 compared with that of fluorine-18 labeled-fluorodeoxyglucose (^{18}F-FDG) in detecting early lung adenocarcinoma (LUAD) remains unknown. Taking the surgical pathology of pulmonary nodule as the gold standard, the diagnostic performance of stage IA LUAD were compared between ^{18}F-FAPI-04 PET/CT and ^{18}F-FDG PET/CT, and the correlation between ^{18}F-FAPI-04 uptake and pathological characteristics of stage IA LUAD.

Methods: This prospective study from February 2023 to October 2023 analyzed patients with stage IA LUAD who underwent simultaneous examinations with ^{18}F-FAPI-04 and ^{18}F-FDG PET/CT. Semi-quantitative parameters such as maximum standardized uptake value (SUVmax), tumor-to-background ratio (TBR), metabolic tumor volume (MTV), total lesion glycolysis (TLG), FAPI avid tumor volume (FTV), and total lesion FAP expression (TLF) were calculated. The two patterns were compared using either a paired Student's *t*-test or a Wilcoxon signed-rank test. Immunohistochemical (IHC) staining for detecting fibroblast activating protein (FAP) expression was performed in all resected tumor specimens. Correlation analysis was performed between ^{18}F-FAPI-04 uptake and pathological features of stage IA LUAD.

Results: A total of 20 patients diagnosed with stage IA LUAD were included in this study. A total of 24 pulmonary nodules were identified in these 20 patients, all of whom were confirmed to have stage IA LUAD through operation and pathology. Of them, 17 nodules were stained by FAP immunohistochemistry. Compared with ^{18}F-FDG, ^{18}F-FAPI-04 PET/CT showed a statistically significant increase in SUVmax and TBR for stage IA LUAD, both in the overall and stratified analyses (adenocarcinoma *in situ* + minimally invasive adenocarcinoma groups *vs.* invasive adenocarcinoma groups; moderately *vs.* well-differentiated lesions; stage IA1 *vs.* IA2+3; P<0.05). The SUVmax of the intense FAP expression group was significantly

higher than that of the mild FAP expression group, demonstrating a statistically significant difference (P=0.005). The FAP-IHC score was positively correlated with the SUVmax of ^{18}F-FAPI-04 (r=0.64, P=0.005).

Conclusions: ^{18}F-FAPI-04 PET/CT demonstrates higher SUVmax and TBR than ^{18}F-FDG PET/CT in the detection of stage IA LUAD. It was re-assured that the ^{18}F-FAPI-04 uptake of stage IA LUAD was positively correlated with the expression of FAP *in vitro*.

Keywords: Lung adenocarcinoma (LUAD); fibroblast activation protein; fluorine 18-labeled fibroblast activation protein inhibitor (^{18}F-FAPI-04); ^{18}F-fluorodeoxyglucose (^{18}F-FDG); positron emission tomography/computed tomography (PET/CT)

Submitted Oct 05, 2024. Accepted for publication Jan 03, 2025. Published online Feb 27, 2025.
doi: 10.21037/jtd-24-1658
View this article at: https://dx.doi.org/10.21037/jtd-24-1658

Introduction

Lung cancer is the leading cause of cancer-related deaths with high rates of morbidity and mortality (1). Most patients are diagnosed at an advanced stage, missing optimal treatment opportunity and increasing the risk of death, particularly in low- and middle-income countries (2). Early detection of lung cancer is crucial for high-risk patients, particularly for identifying stage IA lung cancer. Timely intervention and treatment can enhance a patient's prognosis. Fluorine18-labeled-fluorodeoxyglucose (^{18}F-FDG) positron emission tomography/computed tomography (PET/CT) is widely used for the staging and restaging of lung cancer, as recommended by the National Comprehensive Cancer Network (NCCN) guidelines (3-5). However, false-negative results may occur when evaluating nodules measuring below 1.0 cm (T1a), adenocarcinoma in situ (AIS), or minimally invasive adenocarcinoma (MIA) (6,7). The latter mainly depends on CT morphological diagnosis, but its specificity is not satisfactory, especially for patients with chronic lung diseases, which poses a particular challenge (6).

Researchers have introduced positron-labeled fibroblast activation protein inhibitors (FAPIs) for cancer imaging, targeting fibroblast activating protein (FAP) overexpressed in cancer-associated fibroblasts (CAFs) (8-10). Several studies have confirmed that positron-labeled FAPI PET/CT is superior to ^{18}F-FDG PET/CT in evaluating advanced lung cancers, such as lymph nodes, pleural, liver, and bone metastases. However, its accuracy remains uncertain for early-stage lung adenocarcinomas (LUAD), such as stage IA LUADs (11-14).

Therefore, we aimed to compare the diagnostic value of ^{18}F-FDG PET/CT and ^{18}F-FAPI-04 PET/CT imaging in stage IA LUADs while assessing FAP expression using immunohistochemistry in resected specimens to evaluate the correlation between the uptake levels of ^{18}F-FAPI-04 radiopharmaceuticals and pathological characteristics. We present this article in accordance with the STARD reporting checklist (available at https://jtd.amegroups.com/article/view/10.21037/jtd-24-1658/rc).

Highlight box

Key findings

- The present study revealed a statistically significant increase in the maximum standardized uptake value and the tumor-to-background ratio of fluorine 18-labeled fibroblast activation protein inhibitor (^{18}F-FAPI-04) compared with fluorine-18 labeled-fluorodeoxyglucose (^{18}F-FDG) for stage IA lung adenocarcinoma (LUAD) (P<0.05).

What is known and what is new?

- ^{18}F-FDG positron emission tomography/computed tomography (PET/CT) is used for the staging and restaging of lung cancer, however, false-negative results may occur when evaluating nodules measuring below 1.0 cm (T1a), adenocarcinoma *in situ*, or minimally invasive adenocarcinoma.
- We compared the diagnostic value of ^{18}F-FDG PET/CT and ^{18}F-FAPI-04 PET/CT imaging in stage IA LUADs while assessing fibroblast activating protein (FAP) expression using immunohistochemistry in resected specimens.

What is the implication, and what should change now?

- ^{18}F-FAPI-04 PET/CT may be superior to ^{18}F-FDG PET/CT for detecting stage IA LUAD lesions. ^{18}F-FAPI-04 uptake in stage IA LUAD was significantly and positively correlated with *ex vivo* FAP expression.

Methods

Study design and population

The study was approved by the Clinical Research Ethics Committee of Maoming People's Hospital (No. PJ2023MI-K003-01) and the Declaration of Helsinki (as revised in 2013). All patients provided written informed consent before participating in the study. It was registered at Chictr.org.cn (registration number: ChiCTR2400080737). The surgical pathology of focal lesions was taken as the gold standard, and the receiver operating characteristic curves of the two samples were compared to estimate the sample size. The PASS (version: 11.0.7) software was employed to calculate the sample size, and the subsequent parameters were adopted: power (1 – beta) =0.8, alpha level (significance level) =0.05, and the alternative hypothesis: two-sided test. A total of 56 patients were required.

Inclusion criteria

The inclusion criteria were: (I) age >18 years; (II) Eastern Cooperative Oncology Group (ECOG) score of ≤1; (III) lung nodules ≤3 cm detected on CT scan and had undergone tumor markers examination; (IV) informed consent; and (V) no history of chemotherapy, radiotherapy, or surgical resection before the PET/CT scan.

Exclusion criteria

The exclusion criteria were: (I) lung nodules >3 cm; (II) participants who were pregnant or suspected to be pregnant; (III) interval between ^{18}F-FDG PET/CT and ^{18}F-FAPI-04 inspection >1 week; (IV) more than two primary malignant tumors; and (V) lack of a final histological diagnosis.

Preparation of ^{18}F-FDG and ^{18}F-FAPI-04

^{18}F-FDG and ^{18}F-FAPI-04 were obtained from Dongcheng AMS Pharmaceutical Co., Ltd. (Dongguan, Guangdong, China), utilizing a 20 MeV cyclotron (CYPRIS HM-20, Sumitomo, Kyoto, Japan). Synthesis of the radiotracer ^{18}F-FAPI-04 strictly adhered to the protocol published by Wei *et al.* (15), and the radiochemical purity exceeded 95%.

Patient preparation and ^{18}F-FDG PET/CT protocol

As recommended by the EANM guidelines for tumor imaging in version 2.0, all patients fasted for ≤4 h before ^{18}F-FDG injection for PET/CT scanning (16). Blood glucose levels ≤11 mmol/L (approximately 200 mg/dL) were required before ^{18}F-FDG injection. All patients received manual administration of 4.44 MBq/kg (0.12 mCi/kg) of ^{18}F-FDG, and patients were instructed to lie on the bed. PET/CT acquisition commenced 60±5 min post-^{18}F-FDG injection using a Discovery MI scanner (GE Healthcare, Milwaukee, WI, USA). A low-dose CT scan (120 kV, 80 mA, 3.75-mm thickness) with dose modulation was employed for attention correction and anatomical localization prior to PET imaging. Subsequently, PET data were acquired. PET acquisition ranged from the skull to the upper thigh, requiring five to eight bed positions per patient and two min per bed position. Patients maintained shallow breathing during the PET acquisition. High-resolution breath-hold CT (120 kV, 150 mA, 1.25-mm thickness) scans were acquired for all patients. PET image reconstruction was performed using the Bayesian penalized likelihood algorithm (Q. Clear, GE Healthcare) with a penalization factor (b=750). Attention correction was performed using CT transmission data.

Patient preparation and ^{18}F-FAPI-04 PET/CT protocol

The same patients underwent ^{18}F-FDG and ^{18}F-FAPI-04 PET/CT within 1 week. The patients were advised to refrain from engaging in vigorous physical activity before ^{18}F-FAPI-04 PET/CT, and no additional specific preparations were required. ^{18}F-FAPI-04 PET/CT was performed 1 h after administration of 4.44 MBq/kg (0.12 mCi/kg) of ^{18}F-FAPI-04 following the same operation procedure and imaging analysis as ^{18}F-FDG PET/CT.

Imaging analysis

All acquired data were transferred to an Advantage Workstation (AW version 4.7, GE Healthcare), where attention-corrected PET, CT, and fused PET/CT images (transaxial, coronal, and sagittal) were reviewed and analyzed. Two experienced nuclear medicine physicians (>5 years) independently reviewed all images and were blinded to the medical histories of the participants (X.L. and N.Z.). Any discrepancies were resolved through discussion with a senior expert (>15 years old, H.X.L.). To eliminate intra-observer variability in the quantitative analysis, PET/CT images were quantitatively evaluated by a single nuclear physician (H.X.L.).

The long diameters of the lung nodules were measured

using high-resolution computed tomography (HRCT) images. Any focal accumulation of ^{18}F-FDG or ^{18}F-FAPI-04 exceeding that of the surrounding tissue was interpreted as a positive lesion, indicating suspected malignancy (12). A semi-automatic 3D delineation was utilized to encompass the entire tumor, exhibiting avidity for ^{18}F-FDG or ^{18}F-FAPI-04. A 3D isocontour volume of interest (VOI), established at 41% of the maximum standardized uptake value (SUVmax) threshold, was applied in accordance with the EANM guidelines (16). SUVmax, mean standardized uptake value (SUVmean), and peak standardised uptake value (SUVpeak) within a 1-cm^3 spherical volume were automatically generated. Metabolic tumor volume (MTV) and total lesion glycolysis (TLG), as assessed by ^{18}F-FDG, were documented alongside the corresponding values determined using ^{18}F-FAPI-04 [FAPI avid tumor volume (FTV) and total lesion FAP expression (TLF), respectively].

The uptake of ^{18}F-FDG or ^{18}F-FAPI-04 in the normal lung parenchyma was assessed by using a 2-cm-diameter region of interest (ROI) in the contralateral normal lung parenchyma on the axial slice corresponding to the maximal diameter of the lung nodules. The SUVmean of the normal lung parenchyma was also recorded. The tumor-to-background ratio (TBR) was computed by dividing the SUVmax of the tumor by the SUVmean of the contralateral normal lung parenchyma. The formula is as follows:

$$TBR = \frac{SUV\text{max of tumor}}{SUV\text{mean of contralateral normal lung parenchyma}} \quad [1]$$

Histology and immunohistochemistry

A board-certified and experienced (>10 years) pathologist (Q.W.H.) specializing in oncology who was blinded to the patient's clinical status performed all macro- and microscopic examinations of all surgical specimens. The degree of differentiation in invasive non-mucinous adenocarcinomas was also categorized as moderately or poorly differentiated, based on the 2021 World Health Organization classification of lung tumors (17). The degree of differentiation, tumor size (long-axis diameter), pathological tumor-node-metastasis (TNM) stage (I, II, or III), and tumor stroma ratio (TSR) were documented. The assessment of the TSR was based on previous reports (18,19). Routine microscopic examination of 5-μm hematoxylin-eosin (H&E) stained sections from the primary tumor was analyzed. Utilizing a 5× microscope objective (50× total magnification), the most invasive part of the primary tumor was selected for further evaluation. The region typically comprises two components, the tumor cell component and the stromal component, quantified as percentages.

The percentage of tumor cells within a single field of view was evaluated at 100× magnification within the area, and the remaining percentage was the TSR. For example, the area of tumor cells accounts for 30% of the field of view, 70% of the stromal component, and 70% of the TSR. Calculate the TSR with a value interval of 10% that is, 20%, 30%, and so on. Two to four different fields of view were selected for the evaluation, and the final value was determined based on the highest TSR value. To evaluate the TSR within the tumor, tumor cell infiltration must be present around the stroma within the selected field of view. Areas with more stroma and no tumor cells surrounding the stroma could not be selected for evaluation.

According to the TSR evaluation results, using 50% as the cut-off value, cases with a TSR value higher than 50% were defined as the stromal-rich group, and cases with a TSR value less than or equal to 50% were defined as the stromal-poor group.

Immunohistochemical (IHC) staining was performed to confirm FAP expression in tumor tissues. Surgical specifications were fixed and embedded before sectioning and immunostaining with the FAP-alpha antibody (1:100; ab207178, Abcam, Cambridge, UK). All surgical specimens were stained and analyzed to measure the intensity and percentage of FAP-positive cells. The staining intensity was graded into four classes, and image acquisition was performed using the Mantra multispectral imaging platform.

FAP expression was assessed in cross-sectional areas encompassing tumors and adjacent non-malignant tissues. A semi-quantitative IHC score was determined by the aforementioned pathologist, who evaluated the percentage of FAP-positive cells and their staining intensity under a light microscope at ×10/20 magnification.

The FAP intensity score was graded as zero (none), one (weak), two (intermediate), or three (strong), whereas the semi-quantitative percentages of FAP-positive cells were scored as follows: zero (0%), one (1–25%), two (26–50%), three (51–75%), and four (76–100%). The final FAP-IHC score, which ranged from zero to 12, was calculated by multiplying the intensity and percentage values. Based on this scoring system, tumors were categorized as follows: negative or marked as '0' (IHC score =0), mild or marked as '1' (IHC score between 1 and 4), moderate or marked as '2' (IHC score between 5 and 8), intense or marked as '3' (IHC score between 9 and 12) (20,21).

Table 1 The clinicopathological characteristic of the included patients

Characteristics	Data (N=24)
Age (years)	61.63±10.03
FAPI dose (mCi)	7.27±1.40
FDG dose (mCi)	6.97±1.47
CEA (ng/mL)	2.44±1.56
The long diameter (cm)	1.77±0.65
Gender	
Male	10 (41.7)
Female	14 (58.3)
Smoking status	
Formerly smoked or currently smokes	15 (62.5)
Never smoked	9 (37.5)
Location	
Right lung	11 (45.8)
Left lung	13 (54.2)
Tumor differentiation	
Moderately	14 (58.3)
Well	10 (41.7)
Stage	
IA1	6 (25.0)
IA2	14 (58.3)
IA3	4 (16.7)

Data are presented as mean ± standard deviation or n (%). FAPI, fibroblast activation protein inhibitor; FDG, fluorodeoxyglucose; CEA, carcinoembryonic antigen.

Statistical analysis

All statistical analyses were carried out using R (version 4.3.2) and RStudio (version 2023.12.1 + 402). The normality of all numerical variables was tested by Probability-Probability (PP) plots, and the result distribution was normal or approximately so. All numerical variables were examined through parameter tests. A paired Student's *t*-test was employed to compare paired data. Student's *t*-test was conducted on both groups. The Spearman correlation was utilized for correlation analysis. Continuous variables are presented as mean ± standard deviation (SD), and categorical variables are shown as frequency and percentage. A two-tailed probability value <0.05 was considered statistically significant.

Results

Population

The study included 20 patients, two of whom had two lung nodules each, one had three, and the remaining had one nodule each, for a total of 24 lung nodules. All lung nodules were resected and confirmed to be LUADs by histopathology and immunohistochemistry. However, specimens were not available for six patients (seven lung nodules) who underwent surgery at other hospitals. FAP-IHC staining was performed for the remaining 17 nodules. The patient characteristics are shown in *Table 1*. A flowchart of the research design is presented in *Figure 1*.

Comparison of ^{18}F-FDG and ^{18}F-FAPI-04 uptake in all nodules

The SUVmean of ^{18}F-FAPI-04 was significantly lower than that of ^{18}F-FDG in the contralateral normal lung parenchyma (0.46±0.16 *vs.* 0.50±0.19; P=0.046). On ^{18}F-FDG imaging, the SUVmax, TBR, MTV, and TLG of all tumors were 1.51±0.95, 1.98±1.75, 2.08±2.02, and 2.88±2.83, respectively. On ^{18}F-FAPI-04 imaging, the SUVmax, TBR, FTV, and TLF of all tumors were 3.1±1.55, 4.47±3.75, 2.7±2.14, and 6.37±6.43, respectively. There were significant differences in SUVmax and TBR between ^{18}F-FDG and ^{18}F-FAPI-04 uptake in all tumors (P<0.001, P=0.04 respectively) (*Table 2*). ^{18}F-FAPI-04 PET/CT was easier to observe and diagnose than was ^{18}F-FDG PET/CT for stage IA LUAD, especially AIS and MIA (P=0.001) (*Figure 2*). Moreover, the TLF of ^{18}F-FAPI-04 in the IAC group was significantly higher than those in the AIS and MIA groups (*Table 3*). The TBR of ^{18}F-FAPI-04 was significantly higher than that of ^{18}F-FDG in moderately and well-differentiated lesions (8.76±5.88 *vs.* 4.19±4.03, P=0.001; 5.85±3.84 *vs.* 2.77±2.87, P=0.001). The TBR of ^{18}F-FAPI-04 showed a statistically significant increase compared with ^{18}F-FDG in stage IA1 and IA2+3 (4.47±3.75 *vs.* 1.98±1.75, P=0.04; 8.58±5.34 *vs.* 4.14±3.91, P<0.001) (*Table 2*).

Correlation between ^{18}F-FAPI-04 uptake and histological FAP expression in stage IA LUAD lesions

The FAP-IHC score was 5.59±4.24, and the percentage

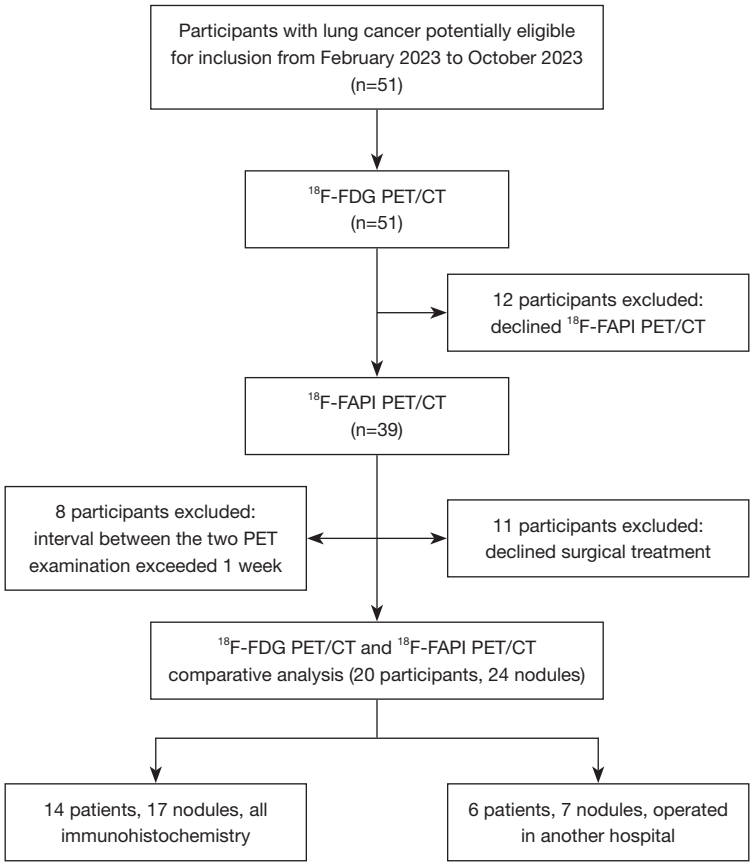

Figure 1 Flowchart of research and design. ^{18}F, fluorine 18; FDG, fluorodeoxyglucose; PET/CT, positron emission tomography/computed tomography; FAPI, fibroblast activation protein inhibitor.

Table 2 Comparison of ^{18}F-FDG and ^{18}F-FAPI-04 uptake in different types of pathological

Characteristics	Value	Tumor size (cm)	SUVmax				TBR			
			FAPI-04	FDG	*t* value	P value	FAPI-04	FDG	*t* value	P value
All lesions	24 (100.0)	1.53±0.64	3.10±1.55	1.51±0.95	5.832	<0.001	4.47±3.75	1.98±1.75	2.736	0.04
Pathological type										
AIS + MIA	9 (37.5)	1.09±0.48	2.07±1.39	0.83±0.38	3.450	0.009	4.74±2.49	1.91±1.14	4.974	0.001
IAC	15 (62.5)	1.71±0.64	3.72±1.31	1.92±0.96	4.770	<0.001	9.23±5.79	4.61±4.18	4.602	<0.001
Differentiation										
Moderately	14 (58.3)	1.82±0.59	3.51±1.38	1.76±0.78	4.723	<0.001	8.76±5.88	4.19±4.03	4.267	0.001
Well	10 (41.7)	1.13±0.47	2.52±1.65	1.17±1.1	3.335	0.009	5.85±3.84	2.77±2.87	5.238	0.001
Stage										
IA1	6 (25.0)	0.78±0.17	1.52±1.14	0.82±0.69	2.874	0.04	4.47±3.75	1.98±1.75	2.736	0.04
IA2+3	18 (75.0)	1.78±0.52	3.63±1.29	1.74±0.92	5.750	<0.001	8.58±5.34	4.14±3.91	5.345	<0.001

Data are presented as n (%) or mean ± standard deviation. P values are for the comparison of ^{18}F-FDG uptake versus ^{18}F-FAPI uptake. ^{18}F, fluorine 18; FDG, fluorodeoxyglucose; FAPI, fibroblast activation protein inhibitor; SUVmax, the maximum standardized uptake value; TBR, the tumor-to-background ratio; AIS, adenocarcinoma in situ; MIA, minimally invasive adenocarcinoma; IAC, invasive adenocarcinoma.

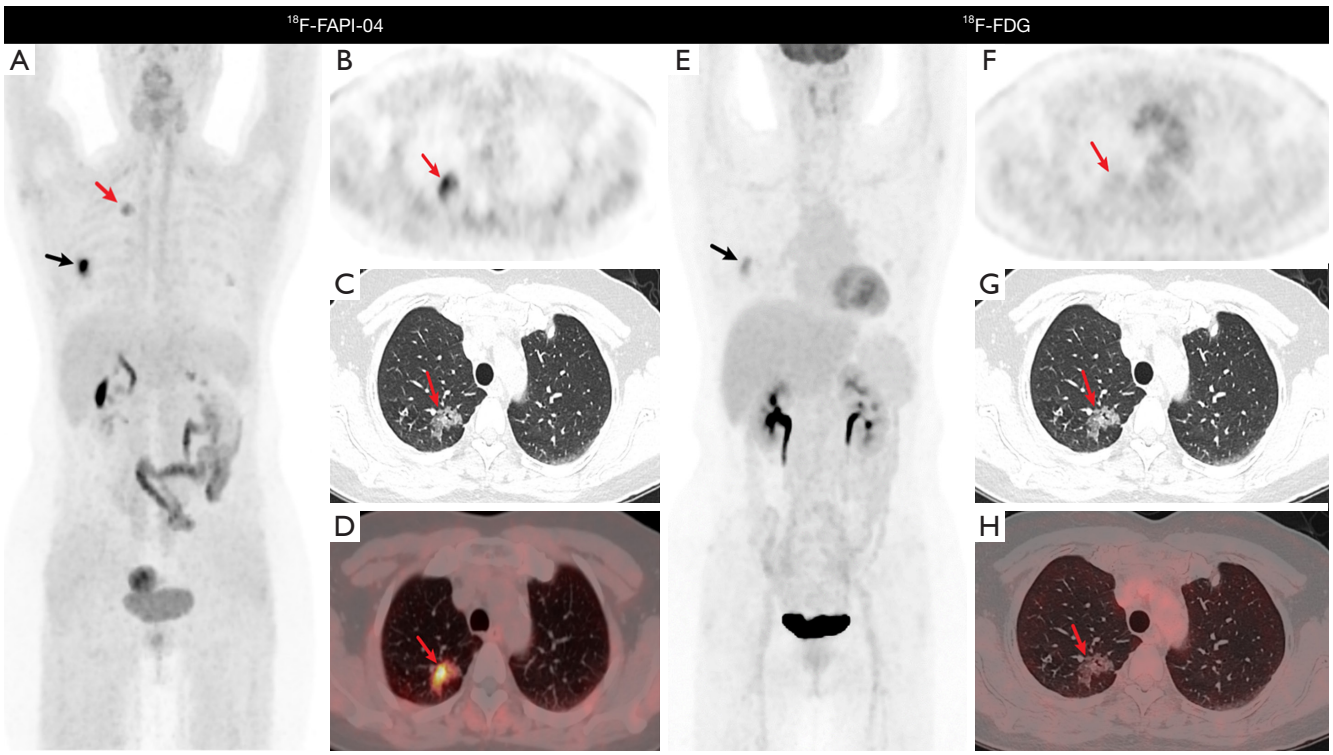

Figure 2 A 58-year-old female (Patient 12) presented with a moderately differentiated invasive adenocarcinoma (1.8 cm in diameter, stage IA2) located in the apical segment of the right upper lobe. (A-D) ^{18}F-FAPI-04 PET/CT images (MIP, PET, CT, and fusion) revealed significantly increased metabolic activity within the lesion (red arrows) (SUVmax =6.0, P<0.05). The TBR was calculated to be 12.0, and the TLF was measured at 14.4 cm^3. (E-H) In contrast, the corresponding ^{18}F-FDG PET/CT images (MIP, PET, CT, and fusion) demonstrated slightly elevated metabolism within the lesion (red arrows; SUVmax =1.6; TBR =2.7; TLF =4.0 cm^3). Additionally, radioactive concentrations are observed in the right rib fracture [black arrows (A) and (E)]. ^{18}F, fluorine 18; FAPI, fibroblast activation protein inhibitor; PET/CT, positron emission tomography/computed tomography; MIP, maximum intensity projection; SUVmax, the maximum standardized uptake value; TBR, the tumor-to-background ratio; TLF, total lesion FAP expression; FDG, fluorodeoxyglucose.

of FAP-positive cells was 53.70%±32.49%. Moderately differentiated stage IA LUAD exhibited significantly increased FAP-IHC score (8.44±3.71, P=0.001) and a higher percentage of FAP-positive cells (76.33±18.16, P<0.001).

The FAP-IHC score of IAC lesions was significantly higher than that of AIS and MIA lesions (7.09±4.48 *vs.* 2.83±1.84, P=0.02). The FAP-IHC score of moderately differentiated lesions was significantly higher than that of well-differentiated lesions (8.44±3.71 *vs.* 2.38±1.77, P=0.001) (*Figure 3*). The SUVmax of ^{18}F-FAPI-04 in the FAP-IHC 1', 2', and 3' groups was 2.68±1.43, 3.44±0.87, and 5.12±1.07, respectively. Notably, the SUVmax of the FAP-IHC 3' group was significantly higher than that of the IHC 1' group, demonstrating a statistically significant difference (P=0.005) (*Figure 4A*).

The optimal threshold of the ^{18}F-FAPI-04 SUVmax for differentiating IAC lesions from AIS and MIA lesions was determined to be 1.3 (*Figure 4B*). The SUVmax of ^{18}F-FAPI-04 of the stromal-rich group (TSR >50%) and the stromal-poor group (TSR ≤50%) was 2.61±1.66 and 4.24±0.88, respectively, with statistically significant differences (P<0.05) (*Figure 4C*). There was no significant difference in the FAP-IHC score between the stromal-rich group (TSR >50%) and the stromal-poor group (TSR ≤50%) (P=0.17). The ^{18}F-FAPI-04 TBR cutoff value for distinguishing IAC lesions from AIS and MIA lesions was established as 5.6 (*Figure 4D*).

FAP was significantly expressed in the stromal cells of LUAD and was found to be expressed in LUAD cells (4/17). PET/CT findings at different FAP expression levels are shown in *Figure 5*.

Table 3 The difference in ^{18}F-FAPI-04 and ^{18}F-FDG PET/CT parameters between different clinic-histopathology groups

Characteristics	N	FAPI SUVmax	FAPI TLF	FDG SUVmax	FDG TLG
Total	24	3.10±1.55	6.37±6.43	1.51±0.95	2.88±2.83
Gender					
Male	10	2.85±1.57	7.65±7.9	1.61±1.09	4.17±3.29
Female	14	3.28±1.56	5.52±5.45	1.44±0.87	1.78±2
t value		0.661	0.717	0.418	1.611
P value		0.52	0.48	0.68	0.14
Age (years)					
<63	12	2.71±1.62	6.15±6.84	1.34±0.8	3.37±3.54
≥63	12	3.49±1.43	6.59±6.36	1.68±1.09	2.32±1.87
t value		1.256	0.148	0.878	0.649
P value		0.22	0.88	0.39	0.53
Location					
Right lung	11	3.54±1.3	7.46±7.33	1.65±0.69	3.15±3.15
Left lung	13	2.73±1.69	5.04±5.23	1.40±1.14	2.28±2.23
t value		1.290	0.828	0.623	0.498
P value		0.21	0.42	0.54	0.63
Size (cm)					
≤1	6	1.52±1.14	1.60±0.85	0.82±0.69	–
>1	18	3.63±1.29	6.90±6.57	1.74±0.92	3.06±2.89
t value		3.553	1.113	2.250	0.750
P value		0.002	0.28	0.04	0.47
Type					
AIS + MIA	9	2.07±1.39	2.42±2.42	0.83±0.38	0.63±0.31
IAC	15	3.72±1.31	7.69±6.86	1.92±0.96	3.56±2.91
t value		2.922	2.536	3.897	1.682
P value		0.008	0.02	0.001	0.12
Grade					
Moderately	14	3.51±1.38	6.68±6.66	1.76±0.78	3.04±3.15
Well	10	2.52±1.65	5.65±6.41	1.17±1.1	2.53±2.34
t value		1.605	0.319	1.538	0.291
P value		0.12	0.75	0.14	0.78
Stage					
IA1	6	1.52±1.14	1.60±0.85	0.82±0.69	–
IA2+3	18	3.63±1.29	6.90±6.57	1.74±0.92	3.06±2.89
F value		12.626	1.239	5.063	0.563
P value		0.002	0.28	0.04	0.47

^{18}F, fluorine 18; FAPI, fibroblast activation protein inhibitor; FDG, fluorodeoxyglucose; PET/CT, positron emission tomography/computed tomography, SUVmax, the maximum standardized uptake value; TLF, total lesion FAP expression; TLG, total 1esion glycolysis; AIS, adenocarcinoma in situ; MIA, minimally invasive adenocarcinoma; IAC, invasive adenocarcinoma.

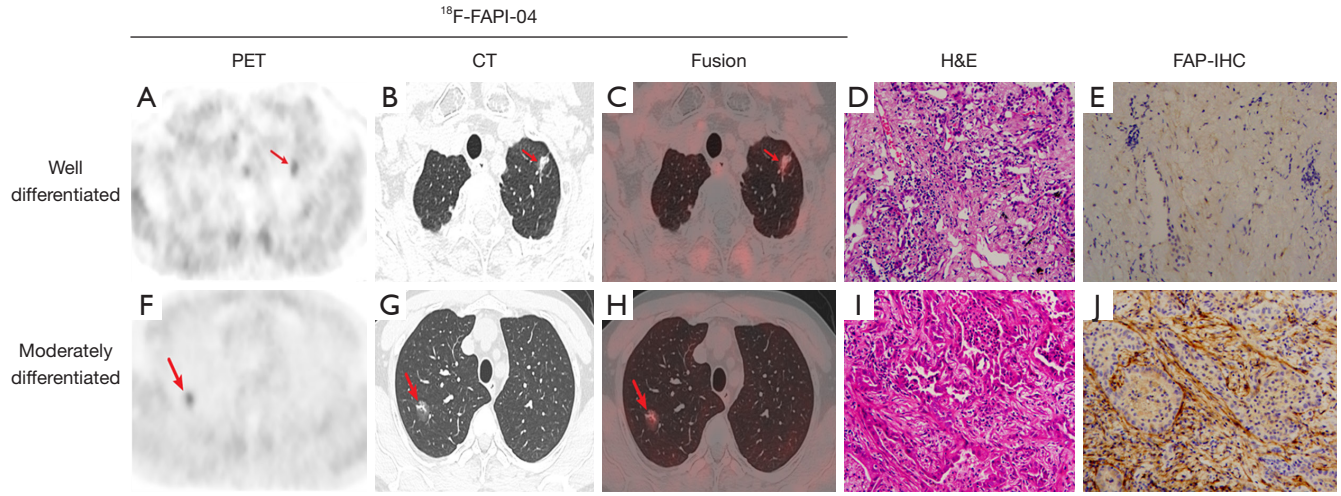

Figure 3 ^{18}F-FAPI-04 PET/CT uptake and FAP-IHC score in well and moderately differentiated types of stage IA LUAD. (A-E) A 76-year-old female (Patient 08) presented with a well-differentiated MIA (diameter 1.5 cm, stage IA2) in the posterior segment of the left superior lobe. (A-C) PET, CT and fusion images revealed slightly increased metabolism of the lesion (red arrows, SUVmax =2.5, TBR =5.0, TLF =1.3 cm^3). (D,E) H&E staining demonstrated the stromal-rich group (TSR >50%), while FAP-IHC exhibited mild expression (IHC score =1', ×20). (F-J) A 51-year-old male (Patient 11) presented with a moderately differentiated IAC (diameter 1.7 cm, stage IA2) in the apical segment of the right upper lobe. (F-H) PET, CT and fusion imaging revealed increased metabolism in the lesion (red arrows, SUVmax =2.9, TBR =7.3, TLF =2.4 cm^3). (I,J) H&E staining indicated the stromal-poor group (TSR ≤50%), and FAP-IHC displayed moderate tumor stroma expression (IHC score =2', ×20). ^{18}F, fluorine 18; FAPI, fibroblast activation protein inhibitor; PET, positron emission tomography; CT, computed tomography; FAP, fibroblast activating protein; IHC, immunohistochemical; LUAD, lung adenocarcinoma; MIA, minimally invasive adenocarcinoma; SUVmax, the maximum standardized uptake value; TBR, the tumor-to-background ratio; TLF, total lesion FAP expression; TSR, tumor-stroma ratio; IAC, invasive adenocarcinoma; H&E, hematoxylin and eosin.

Relationship between ^{18}F-FAPI-04 uptake and tumor clinicopathological feature

The FAP-IHC score positively correlated with the SUVmax of ^{18}F-FAPI-04 (r=0.64, P=0.005). The associations among FAPI SUVmax, FAP expression, and clinicopathological tumor features are shown in *Figure 6*. The differences in ^{18}F-FAPI-04 PET/CT parameters between the different groups are presented in *Table 3*. Variations in FAP-IHC scores across different clinicopathological groups are shown in *Table 4*.

Discussion

The present study revealed a statistically significant increase in the SUVmax and TBR of ^{18}F-FAPI-04 compared with ^{18}F-FDG for stage IA LUAD (P<0.05). This disparity was observed in both pathological subtypes (IAC *vs.* AIS and MIA) and degrees of differentiation (moderately *vs.* well-differentiated). Notably, ^{18}F-FAPI-04 PET/CT is more effective than ^{18}F-FDG PET/CT for diagnosing stage IA LUAD, particularly in cases of AIS and MIA (P=0.001). This may be because stage IA LUAD is a relatively slow-growing cancer of the lungs that is not active in glucose utilization, but the tumor stroma components proliferate rapidly (22). As the tumor grows, it gradually consists of dense tumor cells and tumor stroma, and both FAPI and FDG uptake gradually increase, this is consistent with the results of Zhou *et al.* (23). Understanding the behavior of stage IA LUAD helps in early detection of lesions and treatment planning.

The SUVmax of ^{18}F-FAPI-04 in the stromal-poor group (TSR ≤50%) exhibited a significantly higher value compared with the stromal-rich group (TSR >50%), indicating a statistically significant disparity (P<0.05). The SUVmax of ^{18}F-FAPI-04 in the FAP-IHC 3' group exhibited a significantly higher value compared with the

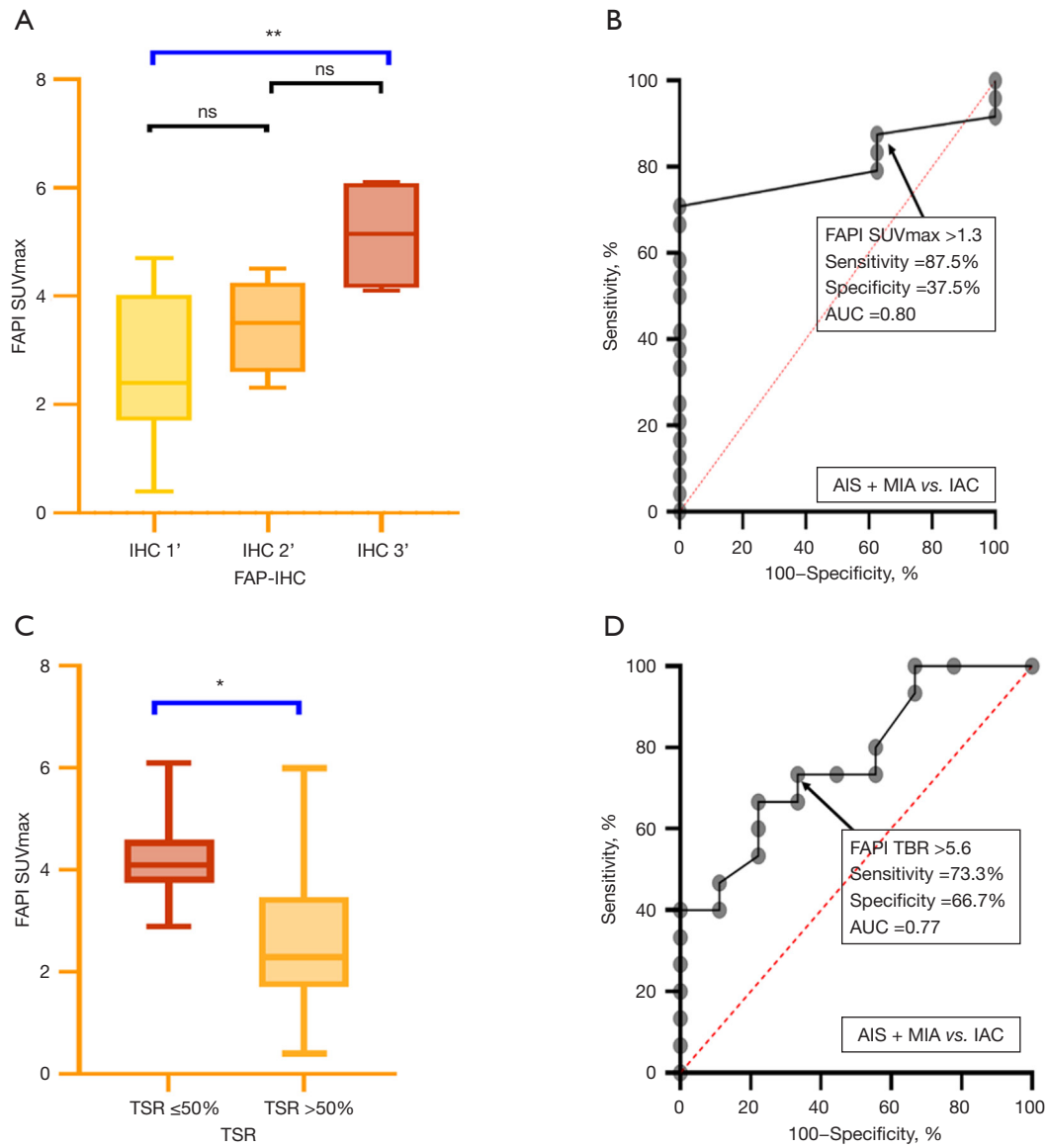

Figure 4 The uptake of ^{18}F-FAPI-04 is significantly higher with higher FAP-IHC scores (3' *vs.* 1') and in stromal-poor tumors compared to stromal-rich tumors, and it demonstrated diagnostic efficacy in differentiating IAC from AIS and MIA. (A) Bar chart demonstrated a significant difference in^{18}F-FAPI-04 SUVmax between FAP-IHC score 1' and 3' groups. (B) The ROC curve represented the diagnostic efficacy of ^{18}F-FAPI-04 SUVmax for differentiating IAC from AIS and MIA. (C) Bar chart showed the difference in ^{18}F-FAPI-04 SUVmax between the stromal-poor group (TSR ≤50%) and the stromal-rich group (TSR >50%). (D) The ROC curve represented the diagnostic efficacy of ^{18}F-FAPI-04 TBR in differentiating IAC from AIS and MIA. Statistical significance was indicated as *, P<0.05; **, P<0.01; ns, not statistically significant. FAPI, fibroblast activation protein inhibitor; SUVmax, the maximum standardized uptake value; FAP, fibroblast activating protein; IHC, immunohistochemical; IHC 1', immunohistochemical; mild or marked as '1'; IHC 2', immunohistochemical, moderate or marked as '2'; IHC 3', immunohistochemical, intense or marked as '3'; AUC, area under the curve; AIS, adenocarcinoma in situ; MIA, minimally invasive adenocarcinoma; IAC, invasive adenocarcinoma; TBR, the tumor-to-background ratio; TSR, tumor-stroma ratio; ^{18}F, fluorine 18; ROC, receiver operating characteristic.

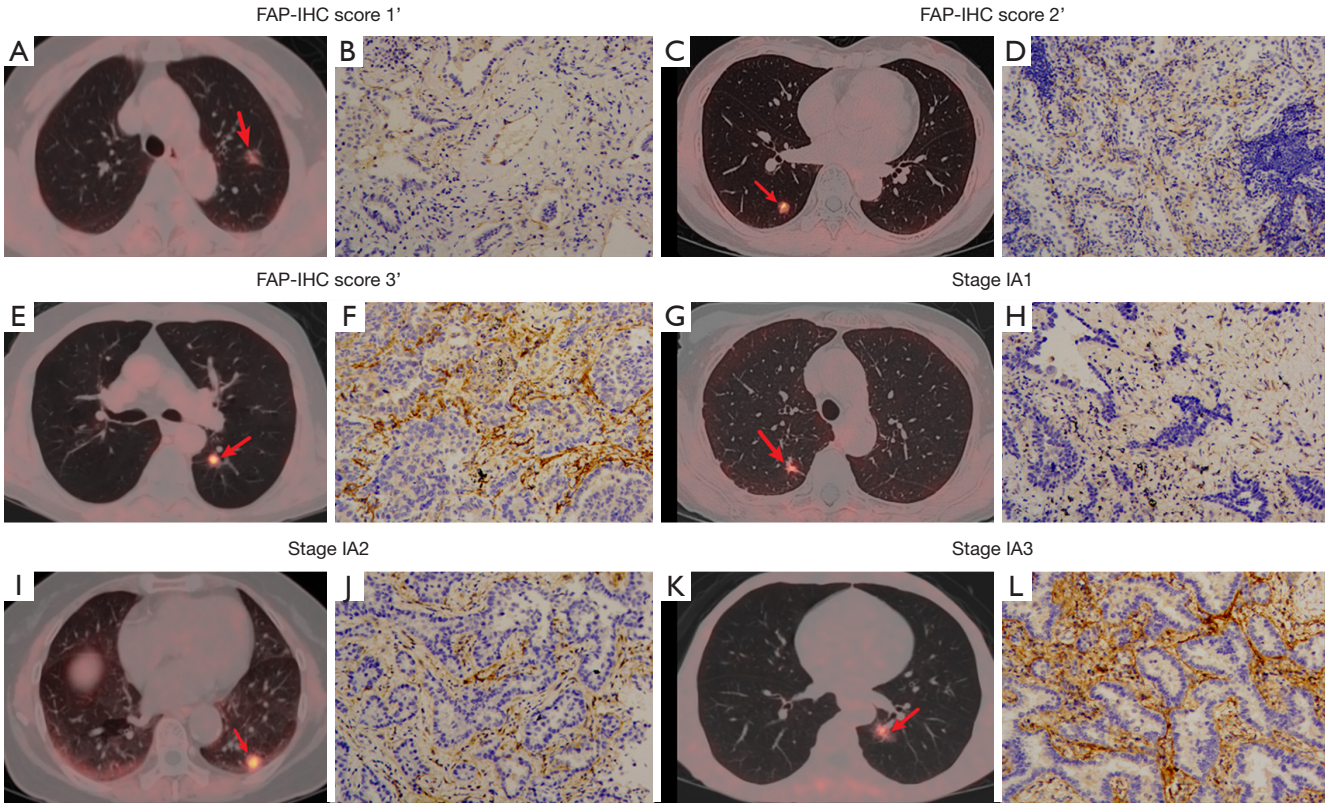

Figure 5 PET/CT findings at different FAP expression levels are shown. (A,B) A 50-year-old male (Patient 02) presents with moderately differentiated IAC located in the posterior segment of the left superior lobe (1.5 cm in diameter, stage IA2). (A) The fusion image from an ^{18}F-FAPI-04 PET/CT scan reveals increased metabolic activity within the lesion (arrow; SUVmax =2.3, TBR =4.6, and TLF =2.8 cm^3). (B) FAP-IHC staining showed mild expression in the tumor stroma (FAP-IHC score =1', ×20). (C,D) A 52-year-old female (Patient 09) with well-differentiated adenocarcinoma AIS located in the posterior basal segment of the right lower lobe (1.1 cm in diameter, stage IA2). (C) The fusion image from an ^{18}F-FAPI-04 PET/CT scan shows increased metabolic activity within the lesion (arrow: SUVmax =4.5, TBR =9.0, TLF =1.3 cm^3). (D) FAP-IHC staining reveals moderate expression in the tumor stroma (FAP-IHC score =2', ×20). (E,F) A 66-year-old male (Patient 14) with moderately differentiated IAC located in the dorsal segment of the left lower lobe (1.2 cm in diameter, stage IA2). (E) The fusion image from an ^{18}F-FAPI-04 PET/CT scan shows increased metabolic activity within the lesion (arrow: SUVmax =4.3, TBR =21.5, TLF =3.5 cm^3). (F) FAP-IHC staining revealed intense expression of FAP in the tumor stroma (FAP-IHC score =3', ×20). (G,H) A 73-year-old female (Patient 03) with a moderately differentiated IAC located in the posterior segment of the right upper lobe (1.0 cm in diameter, stage IA1). (G) The fusion image from an ^{18}F-FAPI-04 PET/CT scan shows increased metabolic activity within the lesion (arrow: SUVmax =3.5, TBR =11.7, TLF =2.2 cm^3). (H) FAP-IHC staining reveals moderate expression in the tumor stroma (FAP-IHC score =2', ×20). (I,J) A 63-year-old female (Patient 05) with moderately differentiated IAC located in the posterior basal segment of the left lower lobe (1.2 cm in diameter, stage IA2). (I) The fusion image from an ^{18}F-FAPI-04 PET/CT scan shows increased metabolic activity within the lesion (arrow: SUVmax =6.1, TBR =8.7, TLF =18.6 cm^3). (J) FAP-IHC staining revealed intense expression of FAP in the tumor stroma (FAP-IHC score =3', ×20). (K,L) A 63-year-old male (Patient 13) with moderately differentiated IAC located in the posterior basal segment of the left lower lobe (2.5 cm in diameter, stage IA3). (K) The fusion image from an ^{18}F-FAPI-04 PET/CT scan shows increased metabolic activity within the lesion (arrow: SUVmax =4.1, TBR =20.5, TLF =4.6 cm^3). (L) FAP-IHC staining revealed intense expression of FAP in the tumor stroma (FAP-IHC score =3', ×20). IHC 1', immunohistochemical; mild or marked as '1'; IHC 2', immunohistochemical, moderate or marked as '2'; IHC 3', immunohistochemical, intense or marked as '3'. PET/CT, positron emission tomography/computed tomography; FAP, fibroblast activation protein; IAC, invasive adenocarcinoma; ^{18}F, fluorine 18; FAPI, fibroblast activation protein inhibitor; SUVmax, the maximum standardized uptake value; TBR, the tumor-to-background ratio; TLF, total lesion FAP expression; IHC, immunohistochemical; AIS, adenocarcinoma in situ.

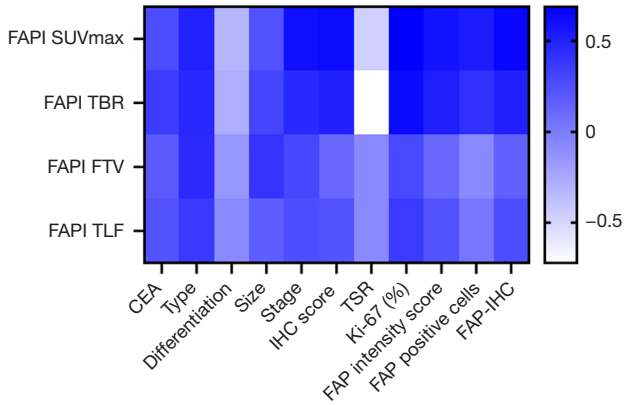

Figure 6 Correlation heat map illustrates the relationship among ^{18}F-FAPI-04 PET/CT imaging parameters, FAP-IHC, and clinicopathological features of stage IA LUAD. FAPI, fibroblast activation protein inhibitor; SUVmax, the maximum standardized uptake value; TBR, the tumor-to-background ratio; FTV, FAPI avid tumor volume; TLF, total lesion FAP expression; CEA, carcinoembryonic antigen; IHC, immunohistochemical; TSR, tumor-stroma ratio; FAP, fibroblast activation protein; ^{18}F, fluorine 18; PET/CT, positron emission tomography/computed tomography; LUAD, lung adenocarcinoma.

FAP-IHC 1' group, a statistically significant disparity (P=0.005). A strong positive correlation was noted between ^{18}F-FAPI-04 uptake and the FAP-IHC score (Spearman's correlation, r=0.64). The findings of this study demonstrate a strong correlation between ^{18}F-FAPI-04 PET/CT uptake and the expression level of FAP, thereby validating the non-invasive visualization capability of this imaging modality for assessing FAP expression.

The degree of FAP expression within the tumor depends on the activation status of fibroblasts, specifically the percentage of stromal content or the quantity of FAP molecules per fibroblast. This is a crucial limiting factor for the detection of tumor lesions. Given that tumor growth beyond 1–2 mm necessitates the development of supportive stroma, FAPI PET/CT can effectively visualise small lesions ranging from 3–5 mm (8).

Our findings indicate that FAP is expressed in stromal and LUAD cells, consistent with previous studies on FAP expression in various tumor cells, including breast cancer cells, pancreatic cancer cells, and oral squamous cell carcinoma cells (24). Shi *et al.* and Ding *et al.* also found that FAP was expressed in pancreatic adenocarcinoma cells (20,25). Further research is required to explore the interactions between tumor cells and CAFs in the tumor microenvironment.

Notably, for the assessment of FAP expression in surgical specimens, we incorporated three parameters, namely the intensity score of FAP, the percentage of FAP-staining positive cells, and the FAP-IHC score. However, the parameter with the strongest correlation was the FAP-IHC score (Spearman correlation, r=0.64), similar to the results reported in the literature (20,26).

The FAP-IHC score for stage IA LUAD varied significantly based on the pathological subtype (IAC *vs.* AIS and MIA; P=0.02) and the degree of differentiation (moderately *vs.* well-differentiated; P=0.001). There was no significant difference in the FAP-IHC score between the stromal-rich group (TSR >50%) and the stromal-poor group (TSR ≤50%) (P=0.17). The number of patients in the stroma-poor group (9/17) was comparable to that in the stroma-rich group (8/17). However, the FAP IHC score of the stroma-rich group was lower than expected, possibly owing to the limited sample size included in this study. Sandberg *et al.* observed that FAP expression was higher in the stroma-rich group (N=9) than in the stroma-poor group (N=16) of colorectal cancer (CRC). Still, the difference was not statistically significant (P >0.05). Sandberg *et al.* attributed this to the fact that the TSR is evaluated in the most invasive part of the tumor, not the entire tumor (27). Zhao *et al.* also found a comparable number of cases in the stroma-poor (72/135) and stroma-rich (63/135) groups among patients with advanced non-small cell lung cancer. Moreover, there was a higher prevalence of high FAP expression in the stroma-poor group, although this difference was not statistically significant (P=0.47) (28).

Limitations

The limitations of this study include its small sample size and lack of IHC information for seven of the 24 lesions. This study specifically focuses on stage IA LUAD and does not include poorly differentiated tumors, thus lacking a systematic analysis of the three pathological differentiation types: well, moderately, or poorly differentiated. Future studies should conduct prospective trials involving larger patient populations.

Conclusions

^{18}F-FAPI-04 PET/CT demonstrates higher SUVmax and TBR than ^{18}F-FDG PET/CT in the detection of stage IA LUAD. It was re-assured that the ^{18}F-FAPI-04 uptake

Table 4 The difference in FAP-IHC between different clinicopathological groups (N=17)

Characteristics	N	Percentage of FAP positive cells (%)			IHC score		
		Value	*t* value	P value	Value	*t* value	P value
Age (years)			0.295	0.77		−0.466	0.65
<63	7	56.57±27.74			5.00±3.79		
≥63	10	51.70±36.79			6.00±4.69		
Gender			−0.094	0.93		0.055	0.96
Male	6	52.67±38.98			5.67±5.24		
Female	11	54.27±30.48			5.55±3.88		
Location			0.001	>0.99		−0.239	0.82
Right lung	7	53.71±32.22			5.29±3.95		
Left lung	10	53.70±34.42			5.80±4.64		
Size (cm)			−0.981	0.34		−1.286	0.22
≤1	4	39.75±29.69			3.25±3.20		
>1	13	58.00±33.20			6.31±4.37		
Type			−1.726	0.11		−2.755	0.02
AIS + MIA	6	36.33±24.06			2.83±1.84		
IAC	11	63.18±33.47			7.09±4.48		
Stage			−0.981	0.34		−1.286	0.22
IA1		39.75±29.69			3.25±3.20		
IA2+3		58.00±33.20			6.31±4.37		
Differentiation			4.548	<0.001		4.209	0.001
Moderately	9	76.33±18.16			8.44±3.71		
Well	8	28.25±25.25			2.38±1.77		

Percentage of FAP positive cells (%): the semi-quantitative percentages of positively stained cells were scored as follows: 0 (0%), 1 (1–25%), 2 (26–50%), 3 (51–75%), and 4 (76–100%). IHC score: the final IHC score was the product of the intensity and percentage value and ranged from 0 to 12. FAP, fibroblast activation protein; IHC, immunohistochemical; AIS, adenocarcinoma in situ; MIA, minimally invasive adenocarcinoma; IAC, invasive adenocarcinoma.

of stage IA LUAD was positively correlated with the expression of FAP *in vitro*.

Acknowledgments

We would like to thank Editage (www.editage.com) for English language editing.

Footnote

Reporting Checklist: The authors have completed the STARD reporting checklist. Available at https://jtd.amegroups.com/article/view/10.21037/jtd-24-1658/rc

Data Sharing Statement: Available at https://jtd.amegroups.com/article/view/10.21037/jtd-24-1658/dss

Peer Review File: Available at https://jtd.amegroups.com/article/view/10.21037/jtd-24-1658/prf

Funding: This work was supported by the funding from the Special Fund Project of Science and Technology in Maoming Guangdong China (No. 2022S001) and the Guangdong Medical Research Fund (No. B2022060).

Conflicts of Interest: All authors have completed the ICMJE uniform disclosure form (available at https://jtd.amegroups.com/article/view/10.21037/jtd-24-1658/coif). The authors have no conflicts of interest to declare.

Ethical Statement: The authors are accountable for all aspects of the work in ensuring that questions related to the accuracy or integrity of any part of the work are appropriately investigated and resolved. The study was approved by the Clinical Research Ethics Committee of Maoming People's Hospital (No. PJ2023MI-K003-01) and the Declaration of Helsinki (as revised in 2013). All patients provided written informed consent before participating in the study.

References

1. Siegel RL, Giaquinto AN, Jemal A. Cancer statistics, 2024. CA Cancer J Clin 2024;74:12-49.
2. Leiter A, Veluswamy RR, Wisnivesky JP. The global burden of lung cancer: current status and future trends. Nat Rev Clin Oncol 2023;20:624-39.
3. Ettinger DS, Wood DE, Aisner DL, et al. NCCN Guidelines® Insights: Non-Small Cell Lung Cancer, Version 2.2023. J Natl Compr Canc Netw 2023;21:340-50.
4. Wang J, Wen X, Yang G, et al. The predictive value of (18)F-FDG PET/CT in an EGFR-mutated lung adenocarcinoma population. Transl Cancer Res 2022;11:2338-47.
5. Guo Y, Zhu H, Chen C, et al. A nomogram based on (18) F-fluorodeoxyglucose PET/CT and clinical features to predict epidermal growth factor receptor mutation status in patients with lung adenocarcinoma. Quant Imaging Med Surg 2022;12:5239-50.
6. Sugawara H, Watanabe H, Kunimatsu A, et al. Adenocarcinoma in situ and minimally invasive adenocarcinoma in lungs of smokers: image feature differences from those in lungs of non-smokers. BMC Med Imaging 2021;21:172.
7. Owens C, Hindocha S, Lee R, et al. The lung cancers: staging and response, CT, (18)F-FDG PET/CT, MRI, DWI: review and new perspectives. Br J Radiol 2023;96:20220339.
8. Loktev A, Lindner T, Mier W, et al. A Tumor-Imaging Method Targeting Cancer-Associated Fibroblasts. J Nucl Med 2018;59:1423-9.
9. Kratochwil C, Flechsig P, Lindner T, et al. (68)Ga-FAPI PET/CT: Tracer Uptake in 28 Different Kinds of Cancer. J Nucl Med 2019;60:801-5.
10. Zukotynski KA, Gerbaudo VH. Understanding the Value of FAPI versus FDG PET/CT in Primary and Metastatic Lung Cancer. Radiology 2023;308:e231768.
11. Wei Y, Cheng K, Fu Z, et al. [18F]AlF-NOTA-FAPI-04 PET/CT uptake in metastatic lesions on PET/CT imaging might distinguish different pathological types of lung cancer. Eur J Nucl Med Mol Imaging 2022;49:1671-81.
12. Wang L, Tang G, Hu K, et al. Comparison of (68)Ga-FAPI and (18)F-FDG PET/CT in the Evaluation of Advanced Lung Cancer. Radiology 2022;303:191-9.
13. Wei Y, Ma L, Li P, et al. FAPI Compared with FDG PET/CT for Diagnosis of Primary and Metastatic Lung Cancer. Radiology 2023;308:e222785.
14. Yang Q, Huang D, Wu J, et al. Performance of [18F] FDG PET/CT versus FAPI PET/CT for lung cancer assessment: a systematic review and meta-analysis. Eur Radiol 2024;34:1077-85.
15. Wei Y, Zheng J, Ma L, et al. [18F]AlF-NOTA-FAPI-04: FAP-targeting specificity, biodistribution, and PET/CT imaging of various cancers. Eur J Nucl Med Mol Imaging 2022;49:2761-73.
16. Boellaard R, Delgado-Bolton R, Oyen WJ, et al. FDG PET/CT: EANM procedure guidelines for tumour imaging: version 2.0. Eur J Nucl Med Mol Imaging 2015;42:328-54.
17. Nicholson AG, Tsao MS, Beasley MB, et al. The 2021 WHO Classification of Lung Tumors: Impact of Advances Since 2015. J Thorac Oncol 2022;17:362-87.
18. Mesker WE, Junggeburt JM, Szuhai K, et al. The carcinoma-stromal ratio of colon carcinoma is an independent factor for survival compared to lymph node status and tumor stage. Cell Oncol 2007;29:387-98.
19. Wang K, Ma W, Wang J, et al. Tumor-stroma ratio is an independent predictor for survival in esophageal squamous cell carcinoma. J Thorac Oncol 2012;7:1457-61.
20. Ding J, Qiu J, Hao Z, et al. Prognostic value of preoperative [68 Ga]Ga-FAPI-04 PET/CT in patients

with resectable pancreatic ductal adenocarcinoma in correlation with immunohistological characteristics. Eur J Nucl Med Mol Imaging 2023;50:1780-91.
21. Henry LR, Lee HO, Lee JS, et al. Clinical implications of fibroblast activation protein in patients with colon cancer. Clin Cancer Res 2007;13:1736-41.
22. Maiga AW, Deppen SA, Mercaldo SF, et al. Assessment of Fluorodeoxyglucose F18-Labeled Positron Emission Tomography for Diagnosis of High-Risk Lung Nodules. JAMA Surg 2018;153:329-34.
23. Zhou X, Wang S, Xu X, et al. Higher accuracy of [68 Ga] Ga-DOTA-FAPI-04 PET/CT comparing with 2-[18F] FDG PET/CT in clinical staging of NSCLC. Eur J Nucl Med Mol Imaging 2022;49:2983-93.
24. Shi J, Hou Z, Yan J, et al. The prognostic significance of fibroblast activation protein-α in human lung adenocarcinoma. Ann Transl Med 2020;8:224.
25. Shi M, Yu DH, Chen Y, et al. Expression of fibroblast activation protein in human pancreatic adenocarcinoma and its clinicopathological significance. World J Gastroenterol 2012;18:840-6.
26. Spektor AM, Gutjahr E, Lang M, et al. Immunohistochemical FAP Expression Reflects (68)Ga-FAPI PET Imaging Properties of Low- and High-Grade Intraductal Papillary Mucinous Neoplasms and Pancreatic Ductal Adenocarcinoma. J Nucl Med 2024;65:52-8.
27. Sandberg TP, Stuart MPME, Oosting J, et al. Increased expression of cancer-associated fibroblast markers at the invasive front and its association with tumor-stroma ratio in colorectal cancer. BMC Cancer 2019;19:284.
28. Zhao Y, Liu Y, Jia Y, et al. Fibroblast activation protein in the tumor microenvironment predicts outcomes of PD-1 blockade therapy in advanced non-small cell lung cancer. J Cancer Res Clin Oncol 2023;149:3469-83.

Cite this article as: Liang HX, Huang QW, He YM, Mai YQ, Chen ZL, Wang BP, Fang N, Hu JF, Li X, Zhang N, Liu ET, Li XC. Comparison of the diagnostic accuracy between ^{18}F-FAPI-04 PET/CT and ^{18}F-FDG PET/CT in the clinical stage IA of lung adenocarcinoma. J Thorac Dis 2025;17(2):661-675. doi: 10.21037/jtd-24-1658